Ca2+ as cofactor of the mitochondrial H+-translocating F1FO-ATP(hydrol)ase

Ca^{2+} as cofactor of the mitochondrial H^+-translocating F_1F_O-ATP(hydrol)ase

Salvatore Nesci, Alessandra Pagliarani

Department of Veterinary Medical Sciences, University of Bologna, Ozzano Emilia Via Tolara di Sopra 50, 40064 Bologna, Italy.

Corresponding author: salvatore.nesci@unibo.it

Running title: H^+-translocation driven by ATP hydrolysis by the Ca^{2+}-activated F_1F_O-ATPase

Abstract

The mitochondrial F_1F_O-ATPase in the presence of the natural cofactor Mg^{2+} acts as the enzyme of life by synthesizing ATP, but it can also hydrolyze ATP to pump H^+. Interestingly, Mg^{2+} can be replaced by Ca^{2+}, but only to sustain ATP hydrolysis and not ATP synthesis. When Ca^{2+} inserts in F_1, the torque generation built by the chemomechanical coupling between F_1 and the rotating central stalk was reported as unable to drive the transmembrane H^+ flux within F_O. However, the failed H^+ translocation is not consistent with the oligomycin-sensitivity of the Ca^{2+}-dependent F_1F_O-ATP(hydrol)ase. New enzyme roles in mitochondrial energy transduction are suggested by recent advances. Accordingly, the structural F_1F_O-ATPase distortion driven by ATP hydrolysis sustained by Ca^{2+} is consistent with the permeability transition pore signal propagation pathway. The Ca^{2+}-activated F_1F_O-ATPase, by forming the pore, may contribute to dissipate the transmembrane H^+ gradient created by the same enzyme complex.

Keywords: Ca^{2+} cofactor; F_1F_O-ATPase; mitochondria; H^+ pump; oligomycin; permeability transition pore; bioenergetics.

1. Introduction

The mitochondrial F_1F_O-ATPase is a multisubunit complex arranged in dimers or oligomers and placed at the edge of the *cristae* of the inner mitochondrial membrane (IMM) [1]. The monomer is formed by two domains, named F_1 and F_O functionally and structurally linked to a stator (lateral stalk) and a rotor (central stalk). The F_1 portion, namely the hydrophilic domain that protrudes in the mitochondrial matrix, has a conspicuous lollipop shape formed by α_3, β_3, γ, δ, and ε subunits. An alternated arrangement of α and β subunits forms a globular hexamer around the γ subunit (Fig. 1A). The structure functions as a reversible rotary molecular motor which can build or hydrolyze ATP depending on the rotation direction, which in turn is driven by the transmembrane proton-motive force (Δp). *In vitro* the γ subunit of F_1-ATPase was shown to rotate within the surrounding $\alpha_3\beta_3$ subunits, synthesizing or hydrolysing ATP in three separate catalytic sites on the α/β subunit interface. The catalytic sites are alternated with the non-catalytic sites, which can only bind adenine nucleotides [2]. During the kinetic reactions, the three non-equivalent conformation β_E (empty), β_{DP} (which hosts ADP) and β_{TP} (contains ATP or ADP) of the catalytic sites, with increasing affinity for ATP, change their conformation and binding properties every 120° with the rotation of the rotor [3]. In addition, the F_1F_O-ATPase catalytic and non-catalytic sites in their different conformations can also bind metal divalent cations [1]. In mammals, the membrane-embedded domain is composed by the *a* subunit, the transmembrane α-helices of *b* subunit, the c_n subunits (n= eight in mammals) which arranged as a cylindric palisade form the *c*-ring, A6L subunit, and the supernumerary subunits *e*, *f*, *g*, DAPIT (Diabetes-Associated Protein in Insulin-sensitive Tissue), 6.8 KDa proteolipid (PL) (Fig. 1A) [4]. The H^+ translocation sector arises from *a/c*-ring interactions by forming two asymmetric half-channels with unexpected horizontal membrane-intrinsic α-helices in the *a* subunit. These two half-channels are mutually offset, while the H^+ binding sites are located on the C-terminal α-helix of each *c* subunit [5]. In the mammalian F_1F_O-ATPase the *a* and A6L membrane subunits are encoded by the mitochondrial DNA. The central stalk within the F_1 domain contains the *γ* subunit, which joined to the *δ* and *ε* subunits, forms a sort of foot which interacts with the loop region of *c*-ring. The lateral or peripheral stalk joins the two F_O and F_1 enzyme domains (Fig. 1A). The *b* subunit spans the complete length of the lateral stalk and interacts with OSCP, F6 and *d* subunits which belong to the soluble

enzyme section. All these subunits connect the soluble stator subunits with α_{TP} subunit of F_1 domain. In addition, the top of α_{TP}, α_{DP}, α_E and the β_{DP} and β_E are only linked with OSCP. Some subunits of the lateral stalk, namely the membrane embedded portion of *b*, *f* and A6L subunits [6] and the supernumerary subunits, are transmembrane subunits [4]. The lateral stalk shows a spectacular flexibility that plays the role of resisting the torque generation of the rotor by coupling F_1 catalysis to H^+ translocation [7,8].

The H^+-translocating F_1F_O-ATPase sustains either ATP synthesis or hydrolysis [9]. In the "forward" mode the Mitchell's proton motive force Δp created by mitochondrial respiration drives ATP formation from ADP and Pi. In the so-called "*reverse*" mode, the phosphorylation potential generated by ATP breakdown is exploited by the enzyme complex to pump H^+ and energize the IMM when the Δp drops [10]. Both ATP synthase and hydrolase activities are opposite F_1F_O-ATPase functions that depend on the bioenergetic state of mitochondria. The bi-functional ATP synthesis/hydrolysis mode coupled to H^+ translocation of F_1F_O-ATPase is a mechanism unique in biology sustained by the natural cofactor Mg^{2+}. The F_1F_O-ATPase can replace Mg^{2+} by Ca^{2+} losing the ATP synthesis function, but preserving the F_1F_O-ATP(hydrol)ase activity [11]. High Ca^{2+} concentrations in mitochondria activate of F_1F_O-ATPase by direct Ca^{2+} binding to the $\alpha_3\beta_3$ globular hexamer that dissociates ATP hydrolysis from H^+ pumping. In this case F_1 was reported to become uncoupled from F_O domain [12]. However, this assumption becomes questionable on considering the recent cryo-EM enzyme structure and structure activity relationship data on the effect of small molecules [13] and specific F_1 and F_O domain inhibitors [11,14]. So, in search for a different interpretation of the findings up to now obtained, experimental and literature data [15] were combined to draw a pattern of the mechanism involved.

2. Materials and Methods

2.1. Preparation of the mitochondrial fractions and F_1F_O-ATPase activity assays

Swine hearts (*Sus scrofa domesticus*) were collected at a local abattoir and transported to the lab. From homogenized heart tissue and then subjected to differential centrifugation [11] the mitochondrial preparations, obtained in a divalent cation-free medium, were characterized as described in [14]. To

evaluate the mitochondrial F_1F_O-ATPase activities, the mitochondrial preparations obtained as described by Nesci et al. [11], were added to the reaction system that contained 3 mM ATP and 2 mM Ca^{2+} or Mg^{2+} in 75 mM ethanolammine–HCl buffer, pH 8.8. The enzyme activity was spectrophotometrically detected and evaluated after subtraction of the non-specific ATP hydrolysis in the blank[16]. The sensitivity of the F_1F_O-ATPase activity, either sustained by Mg^{2+} or by Ca^{2+}, to the specific F_1F_O -ATPase inhibitor oligomycin witnessed the functional and structural coupling between the two sectors F_1 and F_O [14].

2.2. Protein model

The structural details of the protein arrangement in the F_1F_O-ATPase subunits were obtained by the Chem3D program of ChemOffice Professional 19.1.1 software [17] using the deposited structures in PDB.

2.3. Calculations and statistics

In each set of experiments, the data represent the mean ± SD of the number of analyses carried out on at least three distinct mitochondrial preparations. The coupling index was calculated as the ratio between the total F_1F_O-ATPase activity and the oligomycin-sensitive F_1F_O-ATPase activity, being the latter obtained from the difference between the total F_1F_O-ATPase activity and the enzyme activity detected in the presence of 3mg/mL oligomycin, a dose which ensured maximal inhibition of the F_1F_O-ATPase [18].The differences between the enzyme activity data in differently treated mitochondria were evaluated by one way ANOVA followed by Student-Newman-Keuls' test when *F* values indicated significance ($P \leq 0.05$). The significance of the difference between the mean coupling index of the Mg^{2+}-dependent F_1F_O-ATPase and the Ca^{2+}-dependent F_1F_O-ATPase was evaluated by Student's *t* test ($P \leq 0.05$). Percentage data were *arcsin*-transformed before statistical analyses to ensure normality.

3. Results and Discussion

The catalytic and non-catalytic subunits of the F_1F_O-ATPase show specific amino acid residues and secondary structure motifs required for the molecular interaction with adenine nucleotides and divalent cations. An eight amino acids sequence, *GXXXXGKT*, conserved in all ATPases [19] is the basic structural feature of the P-loop, known as a phosphate binding loop, on *α* and *β* subunits (Fig. 1B). The motif interacts with Mg^{2+} and phosphate (Pi) groups of ATP by coordinating β-Pi and γ-Pi to exchange the terminal γ-Pi when the ATP is synthesized or hydrolysed. The positions and specific amino acid composition in the pig sequence are $_{158}$*GGAGVGKT*$_{165}$ and $_{169}$*GDRGTGKT*$_{176}$ in the *β* and *α* subunits, respectively. T_{165} is the only residue that plays a key role in coordinating Mg^{2+} in the *β* subunits of enzyme during ATP hydrolysis, while T_{176} of *α* subunits could bind the cofactor. Similarly to Mg^{2+}, Ca^{2+} can also bind to all the catalytic sites and probably also to the non-catalytic sites [4]. The relative affinities for divalent cations and ATP in the reverse reaction of ATP hydrolysis are modulated by mutagenesis of these specific residues of *β* subunits [20]. However, Ca^{2+}, which has higher steric hindrance than Mg^{2+}, can change the coordination geometry of the Mg^{2+}-binding site from the octahedral bipyramide which binds six ligands up to allow eight ligands when Ca^{2+} is inserted in replacement of Mg^{2+} [21]. Therefore, the rigid octahedral complex changes to a less rigid geometry with irregular bond distances and angles and variable coordination number. This flexible arrangement may explain the non-competitive Ca^{2+} inhibition of the Mg^{2+}-activated F_1F_O-ATPase [14]. The Ca^{2+}-dependent F_1F_O-ATP(hydrol)ase is capable of sustaining torque generation of the rotor. The rotational motion was found to be similar to that induced by Mg^{2+} in the F_1-ATPase [22]. Ca^{2+} binding could have the functional consequence to prevent the building of the transmembrane H^+ gradient, as shown by ACMA fluorescence quenching [23]. However, these results cannot exclude that the rotation driven by ATP hydrolysis stimulated by Ca^{2+} [22] is coupled to H^+ translocation. The Mg^{2+}-activated F_1F_O-ATPase can display H^+ flow across F_O in the absence of adenine nucleotides bound to F_1. This uncoupled proton leakage, known as “proton slip”, is associated with a free-wheeling of the central stalk under non-physiological conditions [10]. In addition, the proton slip is abolished by F_O inhibitors (*e.g.* oligomycin), but it is insensitive to F_1 inhibitors. Conversely, the Ca^{2+}-dependent F_1F_O-ATP(hydrol)ase activity was shown to inhibited by various F_1 inhibitors [14] and insensitive to other Ca-

ATPase inhibitors [24]. Since the F_1F_O-ATPase in the presence of Ca^{2+}shows a four orders of magnitude lower enzyme activity than the Mg^{2+}-activated F_1F_O-ATPase (Fig. 2A), ATP hydrolysis sustained by Ca^{2+} may be unable to support a significant H^+ pumping to energize the membrane. Moreover, the Ca^{2+}-activated F_1F_O-ATPase is now generally recognized to play an important role in the permeability transition pore (PTP) formation and opening [25–29], which can dissipate the Δp [11]. The loss of F_1F_O-ATPase structural-functional integrity emerges as the most likely event involved in the decreased oligomycin sensitivity when the F_1 catalysis is not coupled to H^+ transport by F_O [30]. However, the Ca^{2+}-dependent F_1F_O-ATP(hydrol)ase is inhibited by oligomycin [24]. A similar behaviour was described in pea stem mitochondria, where, since the Ca-ATPase activity was fully sensitive to oligomycin, ATP hydrolysis could be coupled to H^+ translocation [31]. In swine heart mitochondria oligomycin displays a higher inhibition efficiency on the Ca^{2+}-activated F_1F_O-ATPase than on the Mg^{2+}-activated F_1F_O-ATPase, as shown by the lower IC_{50} value (Fig. 2B). The coupling index (the ratio between the total F_1F_O-ATPase activity and the oligomycin-sensitive F_1F_O-ATPase activity) is statistically similar, namely 94.7±1.8% and 91.6±3.7% in presence of Mg^{2+} and Ca^{2+}, respectively. Therefore oligomycin blocks H^+ translocation coupled to ATP hydrolysis irrespective of the divalent cation (Fig. 2C). Consistently, these data suggest that mechanochemical coupling of Ca^{2+}-dependent F_1-ATP(hydrol)ase works as a rotary chemical motor to drive H^+ translocation in the F_O domain [11,16]. The fact that the H^+-pumping activity driven by Ca^{2+} may not energize IMM is not surprising, being supported by the new “bent-pull” model of the *c*-ring gated channel [32] and by the cryo-EM maps of the enzyme exposed to Ca^{2+} [4]. The lack of apparent H^+ translocation with Ca^{2+}-dependent F_1F_O-ATP(hydrol)ase may be rather due to H^+ backflow through the open PTP [33]. Indeed, different Ca^{2+} F_1F_O-ATPase states during ATP hydrolysis were not identified in the Mg^{2+}-activated F_1F_O-ATPase. Moreover recent data show that the PTP opens when the Ca^{2+}-enzyme in disassembled conformation has the peripheral stalk twisted and the F_1 detached from F_O [4] (Fig. 3). In all likelihood, oligomycin inhibits ATP hydrolysis sustained by Ca^{2+} in the first conformational stages of the Ca^{2+}-dependent F_1F_O-ATP(hydrol)ase when F_1 is still coupled to F_O. Indeed, oligomycin, venturicidin, and DCCD, which block H^+ translocation by binding to the *c*-ring, can reduce the calcein quenching rate [34], while small-molecules obtained from the oligomycin structure target

the *c* subunits and inhibit the PTP [35]. Previous experiments in our lab showed that DCCD, which specifically blocks H^+ translocation by covalently binding to the *c* subunit carboxylic groups which constitute H^+ binding sites and inhibits ATP hydrolysis, more promptly reacts and binds to the Ca^{2+}-activated F_1F_O-ATPase than the Mg^{2+}-activated F_1F_O-ATPase [11]. Moreover, in inside-out submitochondrial particles the oligomycin sensitive ATP hydrolysis was shown to be similarly affected by Δ*p* when the enzyme activity is sustained by Ca^{2+} or by Mg^{2+} [11]. Therefore, most likely, when the activating cation is Ca^{2+}, H^+ translocation may be masked by the high ionic conductance of the open PTP.

To sum up, the H^+-translocating Ca^{2+}-dependent F_1F_O-ATP(hydrol)ase is a (mono)functional mode of the mitochondrial F-type ATPase complex. The F_1 domain which hydrolyzes ATP in the presence of Ca^{2+} drives the mechanical-power transmission which results in F_O conductance to H^+. Consistently, the poor H^+-pumping activity of the Ca^{2+}-dependent F_1F_O-ATP(hydrol)ase fails to energize the IMM, mainly because the same enzyme activity is a key PTP constituent, and most likely the PTP opening prevents and masks Δ*p* formation [33,36].

4. Conclusion

Since long-time Ca^{2+} has been involved in the F_1F_O-ATPase modulation in heart mitochondria [37]. Most knowledge comes from *in vitro* experiments, mainly due to difficulties in the detection of individual action mechanisms *in vivo* [38]. The structural data which cast light on the Ca^{2+}-driven conformational changes of the F_1F_O-ATPase shoulder the idea that, among the multiple Ca^{2+} actions in mitochondria, the Ca^{2+} intervention in the PTP is one of the most relevant mitochondrial roles of this multitasking cation in physiology and pathology.

Conflicts of interest

None.

Acknowledgments

This work was supported by the CARISBO Foundation Grants n° 2019.0534, Bologna, Italy to SN.

References

1 Hahn A, Parey K, Bublitz M, Mills DJ, Zickermann V, Vonck J *et al.* Structure of a Complete ATP Synthase Dimer Reveals the Molecular Basis of Inner Mitochondrial Membrane Morphology. *Mol Cell* 2016; **63**: 445–456.

2 Boyer PD. The ATP synthase--a splendid molecular machine. *Annu Rev Biochem* 1997; **66**: 717–749.

3 Yoshida M, Muneyuki E, Hisabori T. ATP synthase--a marvellous rotary engine of the cell. *Nat Rev Mol Cell Biol* 2001; **2**: 669–677.

4 Pinke G, Zhou L, Sazanov LA. Cryo-EM structure of the entire mammalian F-type ATP synthase. *Nat Struct Mol Biol* 2020. doi:10.1038/s41594-020-0503-8.

5 Nesci S, Pagliarani A, Algieri C, Trombetti F. Mitochondrial F-type ATP synthase: multiple enzyme functions revealed by the membrane-embedded FO structure. *Crit Rev Biochem Mol Biol* 2020; : 1–13.

6 Gu J, Zhang L, Zong S, Guo R, Liu T, Yi J *et al.* Cryo-EM structure of the mammalian ATP synthase tetramer bound with inhibitory protein IF1. *Science* 2019; **364**: 1068–1075.

7 Hahn A, Vonck J, Mills DJ, Meier T, Kühlbrandt W. Structure, mechanism, and regulation of the chloroplast ATP synthase. *Science* 2018; **360**: eaat4318.

8 Junge W, Sielaff H, Engelbrecht S. Torque generation and elastic power transmission in the rotary F(O)F(1)-ATPase. *Nature* 2009; **459**: 364–370.

9 Junge W, Lill H, Engelbrecht S. ATP synthase: An electrochemical transducer with rotatory mechanics. *Trends in Biochemical Sciences* 1997; **22**: 420–423.

10 Feniouk BA, Mulkidjanian AY, Junge W. Proton slip in the ATP synthase of Rhodobacter capsulatus: induction, proton conduction, and nucleotide dependence. *Biochim Biophys Acta* 2005; **1706**: 184–194.

11 Nesci S, Trombetti F, Ventrella V, Pirini M, Pagliarani A. Kinetic properties of the mitochondrial F1FO-ATPase activity elicited by Ca(2+) in replacement of Mg(2+). *Biochimie* 2017; **140**: 73–81.

12 Hubbard MJ, McHugh NJ. Mitochondrial ATP synthase F1-beta-subunit is a calcium-binding protein. *FEBS Lett* 1996; **391**: 323–329.

13 Algieri V, Algieri C, Maiuolo L, De Nino A, Pagliarani A, Tallarida MA *et al.* 1,5-Disubstituted-1,2,3-triazoles as inhibitors of the mitochondrial Ca2+ -activated F1 FO -ATP(hydrol)ase and the permeability transition pore. *Ann N Y Acad Sci* 2020. doi:10.1111/nyas.14474.

14 Algieri C, Trombetti F, Pagliarani A, Ventrella V, Bernardini C, Fabbri M *et al.* Mitochondrial Ca2+ -activated F1 FO -ATPase hydrolyzes ATP and promotes the permeability transition pore. *Ann N Y Acad Sci* 2019; **1457**: 142–157.

15 Nesci S, Pagliarani A. Incoming news on the F-type ATPase structure and functions in mammalian mitochondria. *Biochimica et Biophysica Acta - Advances* 2021. doi:10.1016/j.bbadva.2020.100001.

16 Algieri C, Trombetti F, Pagliarani A, Ventrella V, Nesci S. Phenylglyoxal inhibition of the mitochondrial F1FO-ATPase activated by Mg2+ or by Ca2+ provides clues on the mitochondrial permeability transition pore. *Arch Biochem Biophys* 2020; **681**: 108258.

17 Trombetti F, Pagliarani A, Ventrella V, Algieri C, Nesci S. Crucial aminoacids in the FO sector of the F1FO-ATP synthase address H+ across the inner mitochondrial membrane: molecular implications in mitochondrial dysfunctions. *Amino Acids* 2019; **51**: 579–587.

18 Nesci S, Ventrella V, Trombetti F, Pirini M, Pagliarani A. Thiol oxidation is crucial in the desensitization of the mitochondrial F1FO-ATPase to oligomycin and other macrolide antibiotics. *Biochim Biophys Acta* 2014; **1840**: 1882–1891.

19 Ramakrishnan C, Dani VS, Ramasarma T. A conformational analysis of Walker motif A [GXXXXGKT (S)] in nucleotide-binding and other proteins. *Protein Eng* 2002; **15**: 783–798.

20 Du Z, Tucker WC, Richter ML, Gromet-Elhanan Z. Assembled F1-(alpha beta) and Hybrid F1-alpha 3beta 3gamma -ATPases from Rhodospirillum rubrum alpha, wild type or mutant beta, and chloroplast gamma subunits. Demonstration of Mg2+versus Ca2+-induced differences in catalytic site structure and function. *J Biol Chem* 2001; **276**: 11517–11523.

21 Casadio R, Melandri BA. CaATP inhibition of the MgATP-dependent proton pump (H+-ATPase) in bacterial photosynthetic membranes with a mechanism of alternative substrate inhibition. *JBIC* 1996; **1**: 284–291.

22 Tucker WC, Schwarz A, Levine T, Du Z, Gromet-Elhanan Z, Richter ML *et al.* Observation of calcium-dependent unidirectional rotational motion in recombinant photosynthetic F1-ATPase molecules. *J Biol Chem* 2004; **279**: 47415–47418.

23 Papageorgiou S, Melandri AB, Solaini G. Relevance of divalent cations to ATP-driven proton pumping in beef heart mitochondrial F0F1-ATPase. *J Bioenerg Biomembr* 1998; **30**: 533–541.

24 Nesci S, Ventrella V, Trombetti F, Pirini M, Pagliarani A. Preferential nitrite inhibition of the mitochondrial F1FO-ATPase activities when activated by Ca(2+) in replacement of the natural cofactor Mg(2+). *Biochim Biophys Acta* 2016; **1860**: 345–353.

25 Alavian KN, Beutner G, Lazrove E, Sacchetti S, Park H-A, Licznerski P *et al.* An uncoupling channel within the c-subunit ring of the F1FO ATP synthase is the mitochondrial permeability transition pore. *Proc Natl Acad Sci USA* 2014; **111**: 10580–10585.

26 Bonora M, Bononi A, De Marchi E, Giorgi C, Lebiedzinska M, Marchi S *et al.* Role of the c subunit of the FO ATP synthase in mitochondrial permeability transition. *Cell Cycle* 2013; **12**: 674–683.

27 Giorgio V, von Stockum S, Antoniel M, Fabbro A, Fogolari F, Forte M *et al.* Dimers of mitochondrial ATP synthase form the permeability transition pore. *Proc Natl Acad Sci USA* 2013; **110**: 5887–5892.

28 Mnatsakanyan N, Llaguno MC, Yang Y, Yan Y, Weber J, Sigworth FJ *et al.* A mitochondrial megachannel resides in monomeric F1FO ATP synthase. *Nat Commun* 2019; **10**: 5823.

29 Urbani A, Giorgio V, Carrer A, Franchin C, Arrigoni G, Jiko C *et al.* Purified F-ATP synthase forms a Ca2+-dependent high-conductance channel matching the mitochondrial permeability transition pore. *Nat Commun* 2019; **10**: 4341.

30 Devenish RJ, Prescott M, Boyle GM, Nagley P. The Oligomycin Axis of Mitochondrial ATP Synthase: OSCP and the Proton Channel. *J Bioenerg Biomembr* 2000; **32**: 507–515.

31 De Col V, Petrussa E, Casolo V, Braidot E, Lippe G, Filippi A *et al.* Properties of the Permeability Transition of Pea Stem Mitochondria. *Front Physiol* 2018; **9**: 1626.

32 Mnatsakanyan N, Jonas EA. ATP synthase c-subunit ring as the channel of mitochondrial permeability transition: Regulator of metabolism in development and degeneration. *J Mol Cell Cardiol* 2020; **144**: 109–118.

33 Bernardi P, Rasola A, Forte M, Lippe G. The Mitochondrial Permeability Transition Pore: Channel Formation by F-ATP Synthase, Integration in Signal Transduction, and Role in Pathophysiology. *Physiol Rev* 2015; **95**: 1111–1155.

34 Bonora M, Morganti C, Morciano G, Pedriali G, Lebiedzinska-Arciszewska M, Aquila G *et al.* Mitochondrial permeability transition involves dissociation of F1FO ATP synthase dimers and C-ring conformation. *EMBO Rep* 2017; **18**: 1077–1089.

35 Morciano G, Preti D, Pedriali G, Aquila G, Missiroli S, Fantinati A *et al.* Discovery of Novel 1,3,8-Triazaspiro[4.5]decane Derivatives That Target the c Subunit of F1/FO-Adenosine Triphosphate (ATP) Synthase for the Treatment of Reperfusion Damage in Myocardial Infarction. *J Med Chem* 2018; **61**: 7131–7143.

36 Nesci S. The mitochondrial permeability transition pore in cell death: A promising drug binding bioarchitecture. *Medicinal Research Reviews* 2020; **40**: 811–817.

37 Balaban RS. Cardiac energy metabolism homeostasis: role of cytosolic calcium. *J Mol Cell Cardiol* 2002; **34**: 1259–1271.

38 Glancy B, Balaban RS. Role of mitochondrial Ca2+ in the regulation of cellular energetics. *Biochemistry* 2012; **51**: 2959–2973.

Figure 1. Representative structure of F_1F_O-ATPase monomers in mammalian mitochondria (A). The enzyme subunits are drawn as ribbon representations obtained from modified PDB ID codes: 6TT7. Δp, Mitchell's proton motive force, IMM, inner mitochondrial membrane. The letter colors are the same as those of the subunit to which belong. B) Catalytic binding site of F_1F_O-ATPase. The ATP substrate and Mg^{2+} cofactor (in ball and stick representation) are located in the *β* and *α* subunits, drawn as ribbon model (modified PDB ID code: 6J5J) in β_{TP} and α_{TP} conformation, respectively, which show the position of key amino acid residues that bind Mg^{2+}. The P-loop is in light blue in both subunits. The binding sites are viewed from the *γ* subunit (upper panel) and between the observer and the *γ* subunit (lower panel).

Figure 2. Effect of divalent cations on ATP hydrolysis by the mitochondrial F_1F_O-ATPase. A) F-ATPase activities in the presence of Ca^{2+} or Mg^{2+} are shown as bar chart. B) Dose-response curve of oligomycin on the F_1F_O-ATPase activated by Ca^{2+} or Mg^{2+} expressed as percentage of the enzyme activity in the absence of oligomycin. C) The oligomycin-sensitive ATPase activity (▮) and the oligomycin-insensitive ATPase activity in presence of 3 µg/ml of oligomycin (▮) are expressed as percentages of the total mitochondrial ATPase activity sustained by Ca^{2+} or Mg^{2+}, respectively. Data expressed as column chart represent the mean ± SD (vertical bars) from three experiments carried out on different mitochondrial preparations. * indicates significantly different values ($P \leq 0.05$).

Figure 3. F_1F_O-ATPase activity raised by Mg^{2+} or Ca^{2+} as cofactors. ATP hydrolysis sustained by Mg^{2+} (*i*) or Ca^{2+} (*ii*) is coupled to H^+ translocation. The different size of the two cofactors changes the F_1F_O-ATPase conformation. Indeed, the transition of the Ca^{2+}-dependent F_1F_O-ATP(hydrol)ase from the assembled (*ii*) to the disassembled state (*iii*) could induce the loss of H^+-translocation. Consequently, the PTP opens when a retracted *e* subunit pulls the lyso-phophatidylserine plug out of the *c*-ring at the inner mitochondrial membrane side, while the F_1F_O destabilization pulls out phospatidylserine at the matrix side.

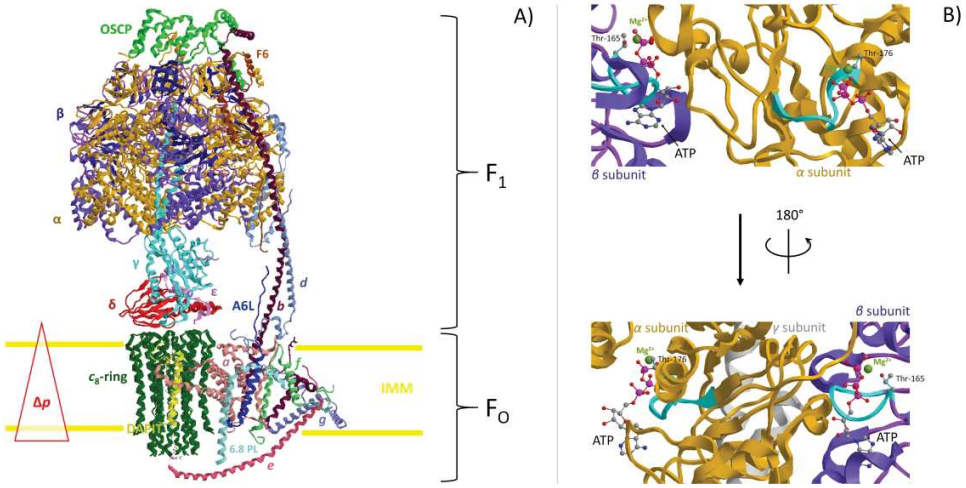

Figure 1. Representative structure of F1FO-ATPase monomers in mammalian mitochondria (A). The enzyme subunits are drawn as ribbon representations obtained from modified PDB ID codes: 6TT7. Δp, Mitchell's proton motive force, IMM, inner mitochondrial membrane. The letter colors are the same as those of the subunit to which belong. B) Catalytic binding site of F1FO-ATPase. The ATP substrate and Mg2+ cofactor (in ball and stick representation) are located in the β and α subunits, drawn as ribbon model (modified PDB ID code: 6J5J) in βTP and αTP conformation, respectively, which show the position of key amino acid residues that bind Mg2+. The P-loop is in light blue in both subunits. The binding sites are viewed from the γ subunit (upper panel) and between the observer and the γ subunit (lower panel).

455x229mm (300 x 300 DPI)

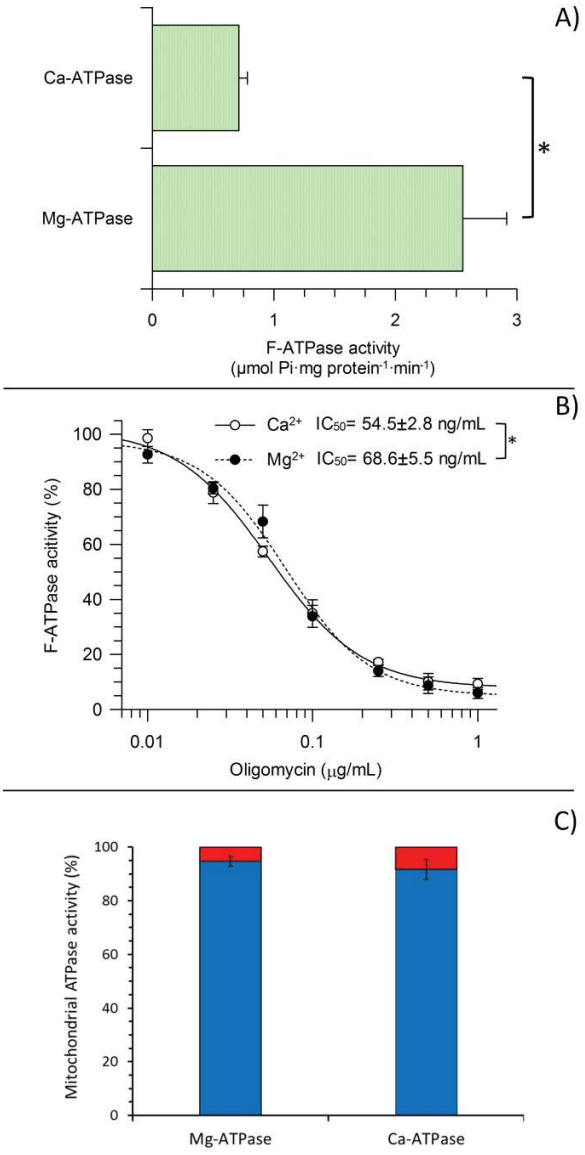

Figure 2. Effect of divalent cations on ATP hydrolysis by the mitochondrial F1FO-ATPase. A) F-ATPase activities in the presence of Ca2+ or Mg2+ are shown as bar chart. B) Dose-response curve of oligomycin on the F1FO-ATPase activated by Ca2+ or Mg2+ expressed as percentage of the enzyme activity in the absence of oligomycin. C) The oligomycin-sensitive ATPase activity (▉ blue) and the oligomycin-insensitive ATPase activity in presence of 3 µg/ml of oligomycin (▉ red) are expressed as percentages of the total mitochondrial ATPase activity sustained by Ca2+ or Mg2+, respectively. Data expressed as column chart represent the mean ± SD (vertical bars) from three experiments carried out on different mitochondrial preparations. * indicates significantly different values (P≤0.05).

100x197mm (600 x 600 DPI)

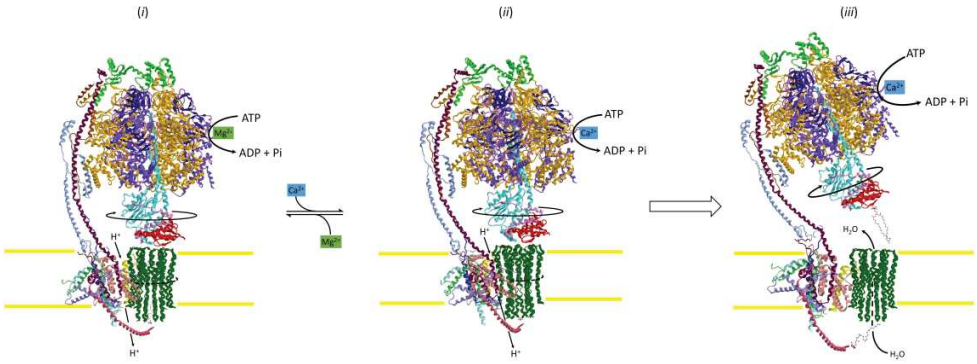

Figure 3. F1FO-ATPase activity raised by Mg2+ or Ca2+ as cofactors. ATP hydrolysis sustained by Mg2+ (i) or Ca2+ (ii) is coupled to H+ translocation. The different size of the two cofactors changes the F1FO-ATPase conformation. Indeed, the transition of the Ca2+-dependent F1FO-ATP(hydrol)ase from the assembled (ii) to the disassembled state (iii) could induce the loss of H+-translocation. Consequently, the PTP opens when a retracted e subunit pulls the lyso-phophatidylserine plug out of the c-ring at the inner mitochondrial membrane side, while the F1FO destabilization pulls out phospatidylserine at the matrix side.

381x143mm (600 x 600 DPI)